Texas A&M University
J. Mike Walker '66 Department of Mechanical Engineering
Turbomachinery Laboratory

A SIMPLE TWO-PHASE FLOW MODEL FOR PREDICTION OF LEAKAGE IN WET GAS LABYRINTH SEALS AND POCKET DAMPER SEALS

TRC-SEAL-03-2020
Research Progress Report to the Turbomachinery Research Consortium

by

Luis San Andrés
Mast-Childs Chair Professor
Principal Investigator

Jing Yang
Assistant Research Engineer

June 2020

TRC Project, TEES # 258124-00027

EXECUTIVE SUMMARY

Current and upcoming two-phase pump and compression systems in subsea production facilities must demonstrate long-term operation and continuous availability. Annular pressure seals, limiting secondary flow, also influence the dynamic stability of turbomachinery. Hence, it is vital to quantify the leakage and dynamic force coefficients of annular seals operating with two-phase flow (gas and liquid mixture). Until now, a time-efficient prediction model such as a bulk flow model (BFM) for labyrinth seals (LSs) and pocket damper seals (PDSs) is not available.

The present work develops a simple flow model predicting the leakage and cavity pressures for LSs and PDSs operating with two-phase flow. The model adapts Neumann's leakage equation for use with the physical properties of a homogeneous two-phase flow mixture.

The developed model predicts the leakage and cavity pressures for a four-blade, eight-pocket fully partitioned PDS operating with a low supply pressure (P_S = 2.3 bar and 3.2 bar) and low rotor speed (5250 rpm, surface speed of 35 m/s). For both the pure gas and wet gas conditions (2.2% in liquid volume), the predicted leakage agrees with the test data. The predicted cavity pressures deviate from computational fluid dynamics (CFD) predictions, in particular for a choked flow condition at P_S = 3.2 bar.

For an eight-blade, eight-pocket fully partitioned PDS supplied with air at a high supply pressure (P_S = 70 bar) and rotor speed at 10 krpm (surface speed = 61 m/s), the model predicted leakage is less than the measured leakage, with a difference less than 14 %. For the PDS supplied with an oil in gas mixture with gas volume fraction = 0.9 ~ 0.98 and exit/inlet pressure ratio = 0.5, the simple model predicted leakage agrees very well with a CFD model predictions. The measured leakage is 33 % larger or than both model predictions; hence likely in error.

Planned follow up work will focus on extending the model toward force coefficients for *wet* gas LSs and PDSs.

TABLE OF CONTENTS

LIST OF TABLES

LIST OF FIGURES

1. INTRODUCTION

By limiting secondary flows, annular pressure seals improve operational efficiency in turbomachinery. The dynamic force characteristics of annular pressure seals also affect the stability and reliability of a rotor-bearing system. Pocket damper seals (PDSs) [1] are a well-known technology (more than 25 years in usage) in modern turbomachinery, in particular in centrifugal compressors.

With the depleting of oil resources, the O&G industry has moved towards (deep) subsea operations. Innovative centrifugal compressors must manage efficiently oil in gas mixtures (*wet* gas) with a liquid volume fraction (LVF) as high as 5%. Recently, the PDS finds an application to *wet* gas compression systems for subsea O&G production facilities. In 2014, Vannini et al. [2] report a severe subsynchronous rotor vibration (SSV) at 45% rotor speed in a single-stage centrifugal compressor, in which a labyrinth seal (LS) operated with a *wet* gas (LVF up to 3%). Replacing the LS with a fully partitioned PDS successfully eliminated the rotor SSV issue. A follow up computational fluid dynamics (CFD) analysis [3] reveals that the (circumferential) partitioning walls in the PDS reduce the accumulated volume in the cavities and decelerate the circumferential fluid flow within a pocket, and which enhance the stability of a rotor-bearing system applied to a *wet* gas operation.

The Turbomachinery Laboratory at Texas A&M University has pioneered in the quantification of leakage and dynamic force coefficients for annular pressure seals operating with two-phase flow (oil and gas mixture). Professor Childs and students constructed a two-phase flow test rig to measure the leakage and dynamic performance of balance piston seals undergoing a large pressure drop and operation at a high rotor speed [4-5]. Zhang et al. [4] test a smooth surface, uniform clearance seal (L/D = 0.65) supplied with a mixture of air and a synthetic oil (PSF-5cSt) with inlet LVF ranging from 0 to 8%. The supply pressure is 62 bar, the pressure ratio PR = discharge pressure/supply pressure = 0.43 ~ 0.57, and the rotor speed is up to 20 krpm (maximum surface speed ΩR = 94 m/s). The seal mass leakage increases by ~ 50% as the inlet LVF increases from 0 to 8% (liquid mass fraction = 51%). The seal direct dynamic stiffnes s coefficient (K) decreases with an increase in liquid volume, except for the condition with PR = 0.43. The seal direct damping coefficient (C) grows with an increase in LVF > 2%, whereas the cross-coupled stiffness (k) increases two to three times as shaft speed grows. The effective damping coefficient ($C_{eff} = C - k$

/ω) grows with an increase in inlet LVF, this demonstrating the liquid viscosity adds substantial damping to the mixture.

In 2019, Delgado and Thiele [6] perform an experimental investigation on an eight-blade, eight-pocket, fully partitioned PDS operating with both air and oil in air mixtures. The authors use Childs' rig [4-5] to conduct tests in a seal having length L = 85.7, diameter = 114.6 mm, and clearance C_r = 0.203 mm. The mixture supply pressure is 70 bar with PR = 0.35, 0.5 and 0.65, and rotor speeds Ω = 10, 15 and 20 krpm (maximum surface speed ΩR = 120 m/s). The gas volume fraction (GVF = 1-LVF) at the seal inlet plane varies from 90% to 100% (pure gas). As the inlet GVF reduces from 100% to 92%, the PDS leakage increases ~ 87% for PR = 0.5. The experimental direct stiffness (K) for the PDS with inlet GVF = 92% is much larger than the test result for operation with pure air (GVF = 1). For instance, the synchronous direct stiffness for the PDS operating with PR = 0.5, rotor speed = 10 krpm and inlet GVF = 92% is ~ 8 MN/m, almost four fold its counterpart with pure gas. The direct damping (C) for inlet GVF = 92% is greater than the one for an inlet GVF = 100% when whirl frequency ω < 200 Hz for operating at three rotor speeds. The direct damping for the PDS supplied with a wet gas consistently decreases with an increase in whirl frequency (ω). The increase of oil volume at the seal inlet reduces the crossover frequency[1] for the test PDS; that is adding liquid in the air enlarges the seal stable operation range.

Besides the test program by Childs, Delgado and their students at the Turbo Lab, San Andrés et al. [7–11] also produce comprehensive experimental results for the leakage and dynamic force coefficients of wet gas annular seals supplied with a mixture of air in ISO VG10 oil. The test seals include a smooth surface annular seal [7-8], a three-wave annular seal [9], step clearance seals [10], and a PDS [11]. The seals' measured mass flow and drag torque enlarge continuously with an increase in the inlet LVF. The force coefficients are frequency dependent for operation with oil and gas mixture.

In Ref. [11], a four-blade, eight pocket fully partitioned PDS is supplied with an oil in air mixture with inlet LVF up to 2.2 %, corresponding to a liquid mass fraction as large as 84%. For tests with a low pressure drop (max. inlet/exit = 3.2) and rotor speed Ω = 5,250 rpm (surface speed ΩR = 35 m/s), the measured leakage for operation with an oil and air mixture is much greater than that with pure air. The difference is due to the large oil density, ~ 728 times greater than air density

[1] The excitation frequency at which the effective damping coefficient ($C_{eff} = C - k/\omega$) changes sign, from negative to positive; typically, a fraction of shaft angular speed.

at ambient conditions. A CFD model with an inhomogeneous Euler method correctly predicts the leakage against the test data. In comparison to operation with only gas, both the test and CFD results demonstrate the PDS has a larger effective damping coefficient, even with a small amount of oil added (LVF = 0.4%),.

In general, there are two numerical methods to analyze the leakage and dynamic performance of *wet* gas annular pressure seals. A CFD analysis provides high-fidelity flow fields, while requiring knowledge to assume the flow structure or type and demanding more computational resources and time than the bulk flow model (BFM). The BFM is simple, fast and efficient, yet its accuracy usually relies on some degree of empiricism. San Andrés [12] and Arghir et al. [13] develop BFMs applicable to homogenous, two-component flows with vastly different physical properties (liquid vs. gas) and analyze the dynamic performance of smooth surface seals and textured seals. In 2019, Grimaldi et al. [14] present a new stratified two-phase bulk flow model to predict the leakage in annular seals. The model assumes the liquid and gas phases flow independently within the seal, i.e. the liquid moves relatively slow (in laminar flow state) and attaches to the stator surface while the gas forms a turbulent flow core in the middle of the seal. The stratified flow model predicted leakage for the smooth seal in Ref. [4] matches better to the test data than the prediction by a homogenous model [12].

Recently San Andrés and Lu [15] develop an inhomogeneous BFM for the prediction of the static and dynamic forced performance of smooth surface, uniform clearance seals. For a high-pressure seal [5] operating with supply pressure = 44.8 bar, discharge pressure = 6.9 bar, and inlet GVF = 0 ~ 0.1, the difference in leakage delivered by both inhomogeneous flow model and a homogenous model is less than 5%. Compared to test results in Ref. [5], both flow models accurately predict the seal direct stiffness drops quickly with inlet GVF, even turning negative. The inhomogeneous flow model does better, however. The two BFMs predict similar cross-coupled stiffness and direct damping coefficients for the high-pressure seal (differences amount to no more than 5%).

Though LSs and PDSs are widely employed in the O&G industry, until now an analytical tool to predict the leakage and dynamic force coefficients for these seal types operating with two-phase flow is not available. The current analysis begins to remedy the situation as it offers a simple, yet accurate, flow model predicting the leakage in *wet* gas supplied LSs or PDSs.

2. A SIMPLE MODEL FOR PREDICTION OF LEAKAGE IN A LABYRINTH SEAL/POCKET DAMPER SEAL SUPPLIED WITH A LIQUID IN AIR MIXTURE

Fluid properties for a two-phase flow model

The following discussion assumes a homogeneous two-phase flow (liquid and gas mixture) through the seal. That is, the liquid and gas components share the same static pressure (P_m) and travel at the same velocity with components W and U along the axial and circumferential directions, respectively. A CFD model assuming an inhomogeneous flow model for analysis of a short PDS [11] finds the fluids' velocity components are identical, i.e., the liquid and gas mixture flowing through the seal is a homogeneous one. Let

$$P_m = P_g = P_l \tag{1}$$

$$W_m = W_g = W_l, \;\; U_m = U_g = U_l \tag{2}$$

where the subscripts m, g, l stand for mixture, gas and liquid.

In a steady state two-phase flow, the gas volume fraction (β) is a function of the supply pressure (P_S) and the gas volume fraction (β_S) at the inlet plane (z=0) [12].

$$\beta = \frac{P_S \beta_S}{P_S \beta_S + (1-\beta_S)P} \tag{3}$$

The mixture density (ρ_m) and the gas mass fraction (λ) equal

$$\rho_m = \beta \rho_g + (1-\beta)\rho_l \tag{4}$$

$$\lambda = \frac{\beta \rho_g}{\beta \rho_g + (1-\beta)\rho_l} = \left[\frac{\rho_g}{\rho_m}\right]\beta \tag{5}$$

There are two formulas to estimate the mixture viscosity (μ_m); one is mass fraction weighted [16] and the other is volume fraction averaged [17].

$$\mu_m = \lambda \mu_g + (1-\lambda)\mu_l \tag{6}$$

$$\mu_m = \beta \mu_g + (1-\beta)\mu_l + 2\sqrt{\beta(1-\beta)\mu_g \mu_l} \tag{7}$$

where μ_g and μ_l are the gas and liquid viscosity, respectively. Based on the two-phase flow analysis by using the two formulas for a smooth surface seal in Ref. [15], Eq. (6) is better for applications of high pressure conditions (i.e., the supply pressure is > 20 bar), and Eq. (7) is more suitable for low pressure applications (say, a few bars).

Based on the recommendation advanced in Ref. [14], the ratio of specific heats (γ_m) for a mixture is

$$\gamma_m = \lambda\gamma_g + (1-\lambda)\gamma_l \tag{8}$$

Above γ_g and γ_l are the specific heat ratios for the gas and liquid, respectively. Further, Ma_m is the Mach number for the mixture defined as

$$\begin{aligned} Ma_m &= \frac{\sqrt{W_m^{\,2} + U_m^{\,2}}}{a_m} \\ \text{with} \quad \frac{1}{a_m} &= \sqrt{\rho_m \left(\frac{\beta}{\rho_g\, a_g^{\,2}} + \frac{1-\beta}{\rho_l\, a_l^{\,2}} \right)} \quad \leftarrow a_g = \sqrt{\gamma_g R_g T}; \quad a_l = \sqrt{\kappa / \rho_l} \end{aligned} \tag{9}$$

where W_m and U_m are the mixture axial velocity and circumferential (cross-film average) velocities at the inlet to the seal. For the homogeneous flow, the mixture axial velocity $W_m = W_g = W_l$ and circumferential velocity $U_m = U_g = U_l$. Above a_g is the sound speed of an ideal (isothermal) gas, a_l is the speed of sound in a liquid with liquid bulk modulus κ, and a_m is the speed of sound in the mixture.

For instance, there is an oil in air mixture with oil density ρ_l = 914 kg/m3, oil dynamic viscosity μ_l = 5.8 cP, and air dynamic viscosity μ_g = 0.0194 cP, under supply pressure P_S = 70 bar and inlet gas volume fraction β_S = 0.75 ~ 0.95. The gas density $\rho_g = P/(R_g \cdot T_S)$, where P is the static pressure and gas constant R_g = 287 J/(kg·K). The operating temperature is constant, T_S = 290 K (17°C). Thus the isothermal gas sound speed a_g = 341.4 m/s. The oil sound speed a_l = 1470 m/s as the oil bulk modulus $\kappa = 1.98\times10^9$ kg/(m·s).

Figure 1 displays the gas volume fraction (β) and gas mass fraction (λ) by Eq. (3) and Eq. (5) for the pressure drop from P_S = 70 bar to P_a = 21 bar. β linearly increases with the drop of pressure (P). λ is independent of the pressure variation within the seal.

Figure 2 depicts the oil in air mixture density (ρ_m) versus the pressure variation. ρ_m reduces consistently as pressure P decreases. Note the oil density is much larger than the gas density, ρ_l / ρ_g ~ 36 for P_a = 21 bar. Therefore, the mixture density grows with a decrease in β_S, for there is more oil added into the mixture at the inlet.

Figure 3 shows the mixture dynamic viscosity (μ_m) calculated by the two formulas, Eq. (6) and Eq. (7), assuming the oil viscosity and air viscosity are invariants in present analysis. The mass weighted mixture viscosity by Eq. (6) is a constant through the seal. The volume weighted viscosity by Eq. (7) for the mixture decreases with the reduction of pressure P. The volume-weighted viscosity is smaller than the mass weighted ones. Recall μ_l / μ_g ~ 299. The oil viscosity

μ_l dominates the calculation of mixture density. Thus, the mass weighted μ_m > the volume weighted μ_m for liquid mass fraction (1 - λ) >> liquid volume fraction (1 - β).

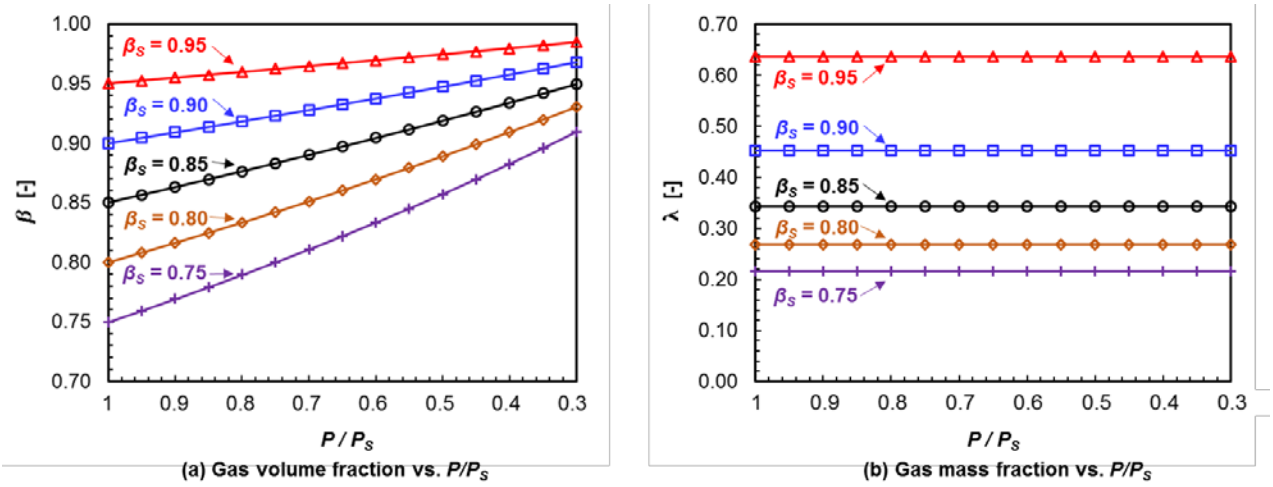

Figure 1. Gas volume fraction (β) and gas mass fraction (λ) versus pressure (P/P_S) for inlet gas volume fraction β_S = 0.75 ~ 0.95. Supply pressure P_S = 70 bar, discharge pressure $P_a = 0.3P_S$ = 21 bar.

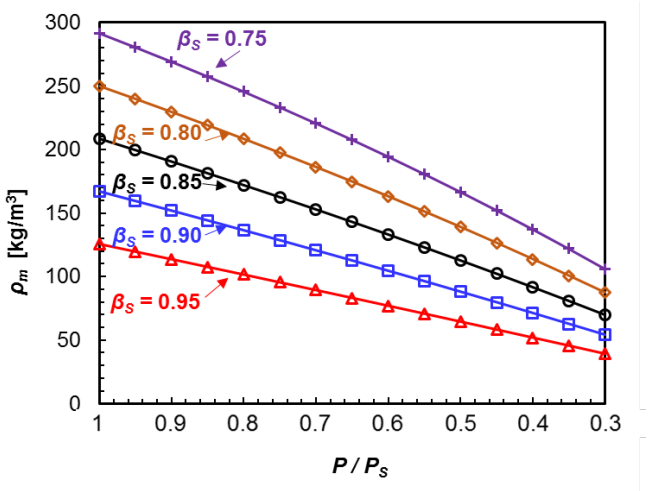

Figure 2. Oil and air mixture density (ρ_m) versus pressure (P/P_S) for inlet gas volume fraction β_S = 0.75 ~ 0.95. Supply pressure P_S = 70 bar, discharge pressure $P_a = 0.3P_S$ = 21 bar.

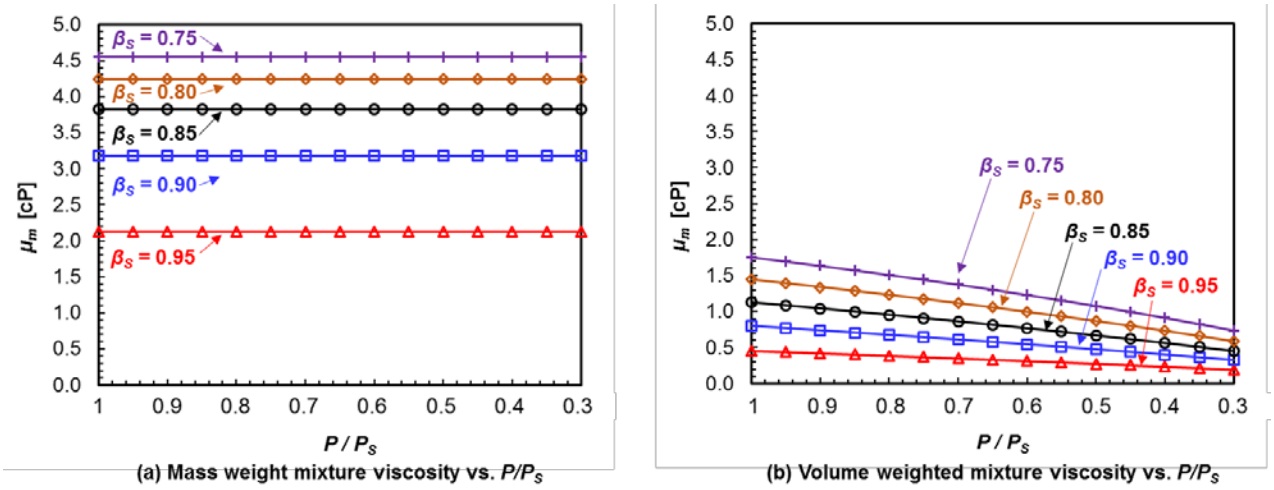

Figure 3. Oil and air mixture (a) mass weight viscosity and (b) volume weight viscosity versus pressure (P/P_S) for inlet gas volume fraction β_S = 0.75 ~ 0.95. Supply pressure P_S = 70 bar, discharge pressure $P_a = 0.3P_S$ = 21 bar.

Figure 4 displays the ratio of specific heats (γ_m) for the oil and air mixture. γ_m drops as the inlet gas volume fraction β_S decreases. From β_S = 0.95 to 0.75, γ_m reduces from 1.38 to 1.30. Figure 5 depicts the variation of mixture sound speed (a_m) versus the pressure. a_m decreases with the pressure P, which indicates the compressibility of mixture enhances with adding oil into the air. For β_S = 0.95, a_m = 286.6 m/s for P_S = 70 bar drops to 276.6 m/s for P/P_S = 0.3 (~ 3% decrease). With adding more oil at inlet (decrease of β_S), the difference of sound speed at seal inlet and outlet grows larger, drops ~ 17% for β_S = 0.75.

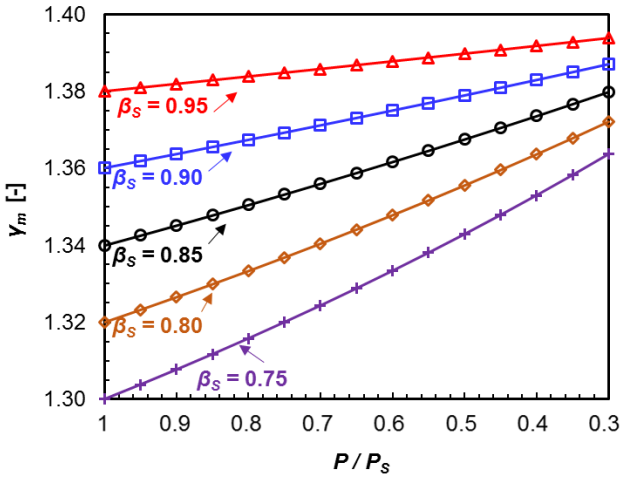

Figure 4. Oil and air mixture specific heat ratio (γ_m) versus pressure (P/P_S) for inlet gas volume fraction β_S = 0.75 ~ 0.95. Supply pressure P_S = 70 bar, discharge pressure $P_a = 0.3P_S$ = 21 bar.

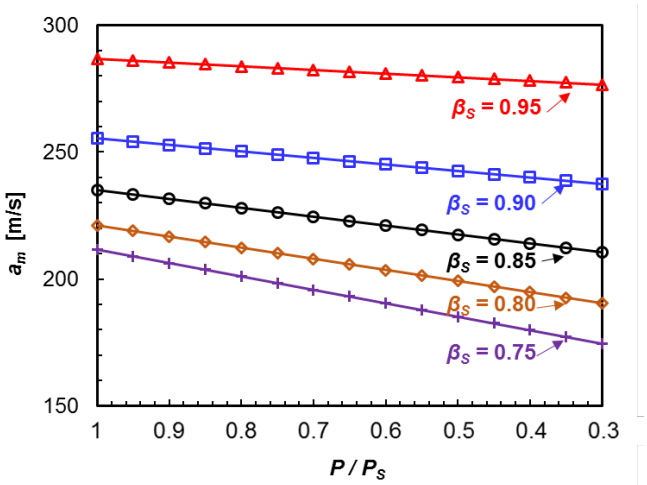

Figure 5. Oil and air mixture sound speed (a_m) versus pressure (P/P_S) for inlet gas volume fraction β_S = 0.75 ~ 0.95. Supply pressure P_S = 70 bar, discharge pressure $P_a = 0.3P_S$ = 21 bar.

Mass flow of a gas through a restriction blade

Figure 6 displays a schematic cross-section plane for a pocket damper seal. Note the graphical depiction also applies to a labyrinth seal, in which cavities replace the pockets shown in the figure. The seal has N blades (*rib*s) along the axial direction. Let P_i stands for the average (cross-film) pressure in the i_{th} pocket or cavity. P_1 is the supply pressure ($P_1 = P_S$) and P_{N+1} is the discharge pressure ($P_{N+1} = P_a$). $\dot{m}_i$ represents the mass flow rate below the i_{th} rib or blade, and based on Neumann's equation [18] equals

$$\dot{m}_i = \mu_{ci}\mu_{fi}\left(\pi DC_r\right)\rho_i W_i \tag{10}$$

where μ_{ci} is a kinetic energy carry-over coefficient, μ_{fi} is a flow discharge coefficient (i = 1, …, N). Derived directly from Bernoulli's equation for an ideal gas,

$$\rho_i W_i = \sqrt{2\rho_i(P_i - P_{i+1})} = \sqrt{\frac{\left(P_i + P_{i+1}\right)}{R_g T}\left(P_i - P_{i+1}\right)} \tag{11}$$

which assumes an average density. Above R_g is the specific gas constant (R_g = 287.15 J/(kg·K) for air) and T is the absolute temperature.

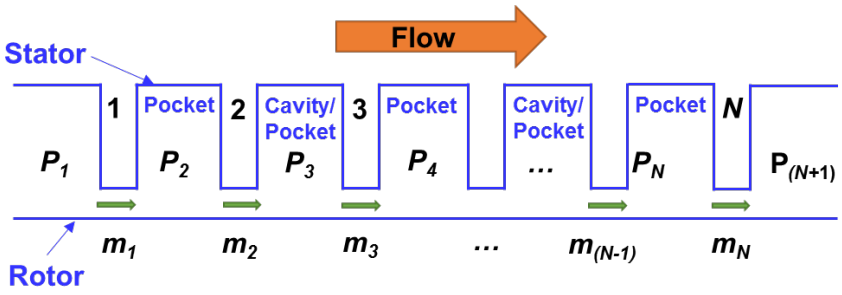

Figure 6. Schematic cross-section plane of a pocket damper seal. (not to scale)

The kinetic energy carry-over coefficient (μ_{ci}) is a correction factor that the gas stream forms into a jet after passing below the first tooth in the seal. μ_{ci} is a function of the seal tip clearance (C_r) and cavity length (L_C) [19],

$$\mu_{ci} = \begin{cases} 1 \quad (i=1) \\ \sqrt{\dfrac{N}{(1-\eta)N+\eta}}; \ \eta = 1 - \dfrac{1}{(1+16.6C_{ri}/L_{Ci})^2} \quad (i \geq 2) \end{cases} \tag{12}$$

where C_{ri} is the clearance below the i-th blade or rib, and L_i is the axial length of the (i+1)-th cavity. For a typical eight-blade, eight pocket PDS, (C_r / L_C) = 0.02, then η = 0.44 and μ_{ci} = 1.27. If C_r / L_C → 0, then η → 0 and μ_{ci} → 1.

The flow discharge coefficient (μ_{fi}) represents a contraction factor accounting of the Vena contracta effect for the fluid after flowing through a restriction and expanding into a cavity. The Chaplygin's equation to calculate μ_{fi} is [19]

$$\mu_{fi} = \frac{\pi}{\pi + 2 - 5S_i + 2S_i^2}; \quad S_i = \left(\frac{P_i}{P_{i+1}}\right)^{\frac{\gamma-1}{\gamma}} - 1 \tag{13}$$

Figure 7 displays the flow discharge coefficient (μ_f) versus pressure ratio (P_i/P_{i+1}) with air as the gas.. If P_i/P_{i+1} approaches 1, $\mu_{fi} \sim \pi / (\pi+2) = 0.61$.

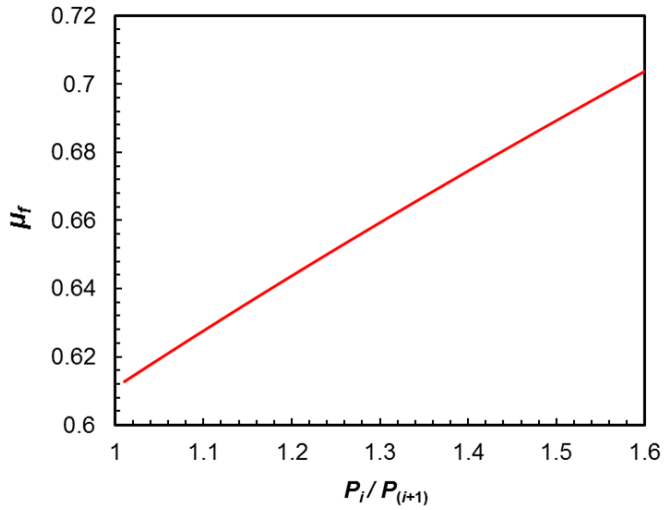

Figure 7. Flow discharge coefficient (μ_f) versus pressure ratio (P_i / P_{i+1}). For air, flow is choked when (P_i / P_{i+1}) ≥ 1.9.

Mass flow of a mixture through a restriction blade

For a mixture flowing through a restriction, and similar to the flow of an ideal gas, consider

$$\left(\rho_m W_m\right)_i = \sqrt{2\rho_{m_i}\left(P_i - P_{i+1}\right)} \tag{14}$$

Eq. (14) is just Bernoulli's equation for an inviscid[2] (ideal) fluid. Substituting Eq. (3) and Eq. (4) into Eq. (14), and after algebraic manipulation, one obtains

$$\left(\rho_m W_m\right)_i^2 = (P_i^2 - P_{i+1}^2)\left[\frac{2\rho_{m_S}}{2\beta_S P_S + (1-\beta_S)(P_i + P_{i+1})}\right] \tag{15}$$

Therefore the mass flow rate below a tooth is

$$\dot{m}_i = \left(\pi D C_r\right)\mu_{ci}\,\mu_{fi}\sqrt{\left(P_i^2 - P_{i+1}^2\right)\left[\frac{2\rho_{m_S}}{2\beta_S P_S + (1-\beta_S)(P_i + P_{i+1})}\right]} \tag{16}$$

where (for simplicity)the original correction factors (μ_{ci} , μ_{fi}) are kept.

Boundary conditions

The mixture supply pressure (P_S) and discharge pressure (P_a) are known at the seal inlet plane and outlet plane ($z = L$). The inlet circumferential velocity at (z=0) is $U_m = \alpha\,(\Omega R)$, where α is an

[2] The model is clearly not valid for a slow flow condition as that produced by a significant content of liquid with viscosity $\mu_l >> \mu_g$.

inlet pre-swirl ratio and (ΩR) is the rotor surface speed. $\alpha \sim 0.50$ for a 50% inlet pre-swirl condition.

Figure 8 displays a schematic diagram for a seal with an upstream cavity and a graph of the pressure variation along the flow direction. Due to a vena contracta effect, the static pressure at the seal inlet plane is $P_e < P_S$. For a compressible flow, Arghir and Frene [20] define a formula to calculate P_e as

$$P_e = P_S \left[1 + \left(\frac{\gamma_m + 1}{2} \right) (1 + \zeta) Ma_m^{\,2} \right]^{\gamma_m / (1-\gamma_m)} \tag{17}$$

where ζ is an (empirical) inlet loss coefficient. Recall Eqs. (8) and (9) for the calculation of the mixture specific heat ratio (γ_m) and the Mach number for the mixture (Ma_m).

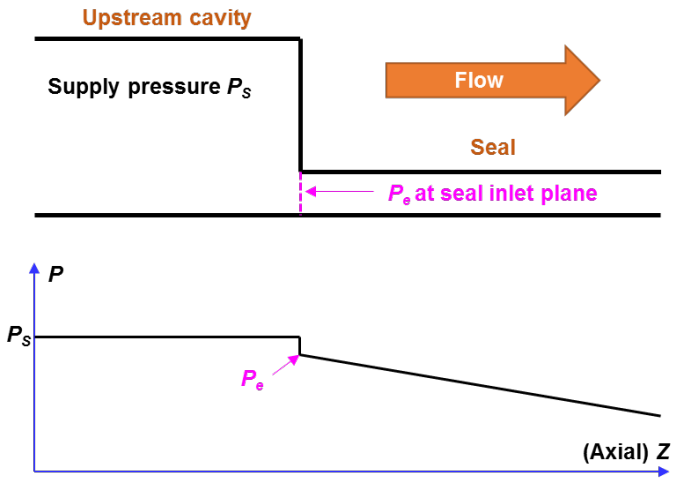

Figure 8. A schematic diagram showing a seal with an upstream cavity and the variation of static pressure along the flow direction. (Not to scale)

3. RESULTS AND DISCUSSION

Validation 1. Leakage for a PDS operating with a low pressure drop

A computational program uses the equations above to predict the leakage and cavity pressures for a four-blade, eight-pocket PDS [11] with geometry and operating conditions listed in Table 1. The PDS operates with a supply pressure as high as 3.2 bar, discharge pressure = 1 bar, and rotor speed of 5250 rpm (surface speed 35 m/s), similar to the operating condition for a pump neck-ring seal. For the current prediction, the inlet loss coefficient is assumed as $\zeta = 0.1$.

Figure 9 displays the predicted and measured leakage for the PDS operating with just air (GVF = 1) versus a pressure ratio (P_S/P_a). The predicted leakage agrees with the test data. Figure 10 shows the predicted cavity pressures and the CFD predicted static pressure along the axial direction. For Ps = 2.3 bar, the code predicted cavity pressure is slightly lower than the CFD results. Whereas for Ps = 3.2 bar, the predicted cavity pressure is lower than the CFD prediction, in particular at pockets #1 and #3. For pocket #3, the predicted pressure P_4/P_a = 1.63, different from the CFD prediction (P_4/P_a = 1.99, choked flow condition). The predicted cavity pressures are similar to the prediction in Ref. [11] and based on the BFM introduced by [21].

Table 1. Geometry and operating conditions of a four-rib fully partitioned pocket damper seal operating with air and an oil in air mixture. From Ref. [11].

Seal length, L	48 mm
Rotor diameter, $D_r = 2R_r$	127 mm
Stator diameter, D_s	137 mm
Clearance height, C_r	0.184 mm
Number of *ribs*	4 (axial)
Number of partition walls (ridges)	8 (circumferential, 45º)
Pocket length, L_C	10.5 mm / 4.8 mm
Pocket depth, d	4.8 mm
Rib axial thickness, δ_{rib}	2.5 mm
Working fluid	Oil in air mixture
Supply pressure, P_S	1.6, 2.3, 3.2 bar(a)
Exit pressure, P_e	1 bar(a)
Supply temperature, T_S	315 K
Air density at (P_S, T_S), ρ_g	1.14 kg/m^3
Air viscosity at (P_S, T_S), μ_g	1.8×10^{-5} kg/(m·s)
Oil density, ρ_l	830 kg/m^3
Oil viscosity at (P_S, T_S), μ_l	8.2 cP
Rotor speed, Ω	5,250 rpm
Surface speed, ΩR	35 m/s
Liquid volume fraction	0, 0.4%, 2.2%

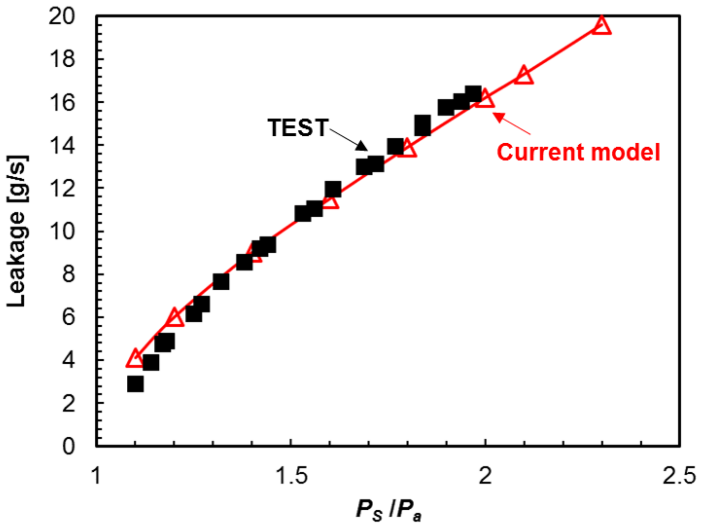

Figure 9. Predicted (current model) and measured (test) leakage for a PDS vs. (P_S / P_a). Rotor speed = 5250 rpm (surface speed = 35 m/s). Test data from Ref. [11].

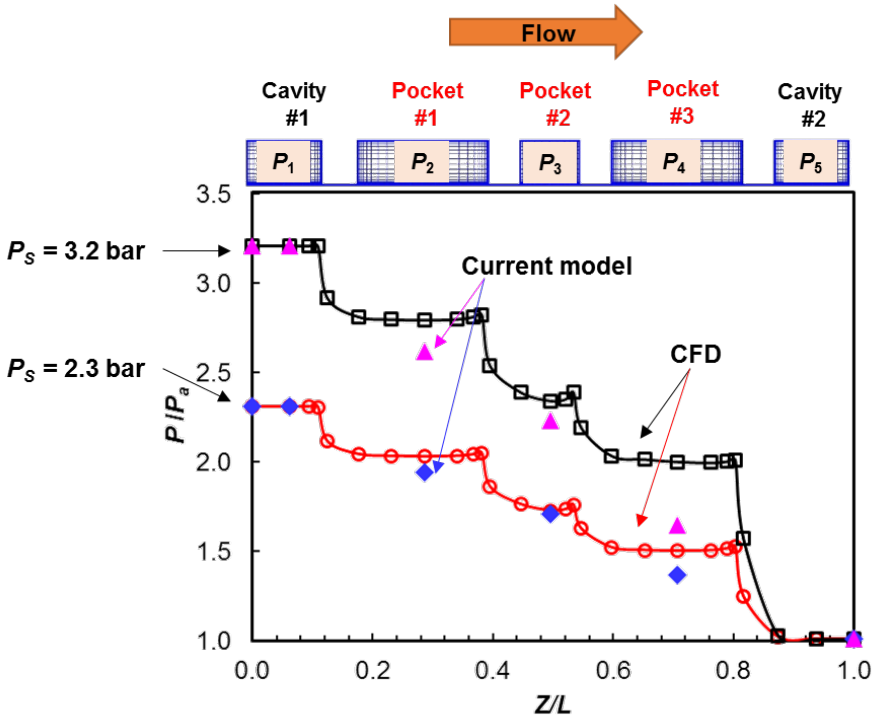

Figure 10. PDS predicted (current model) cavity pressures and CFD static pressure vs. flow direction (z/L). Supply pressure P_S = 2.3 bar and 3.2 bar, rotor speed = 5250 rpm (surface speed = 35 m/s). CFD results from Ref. [11].

Validation 2. Leakage for a PDS operating at a low supply pressure and supplied with an oil in air mixture

For the PDS in Table 2 and supplied with a silicone oil (ISO-VG10) in air mixture, Table 2 lists the predicted leakage for operation with supply pressure P_S = 2.3 bar and inlet liquid volume fraction LVF= 0.4% (β_S = 99.6 %), and with supply pressure P_S = 3.2 bar and inlet LVF = 2.2% (β_S = 97.8%). The experimental and CFD results are from Ref. [11]. For the two operating conditions, the current model prediction of leakage agrees extremely well with the measurement and CFD results. The table includes the mass flow content for the two components, air and gas. Note that an inlet LVF=2.2 % corresponds to a large liquid mass fraction at ~ 84%.

Table 2. Current model predicted leakage and measured (test) and CFD leakage for a PDS operating with an oil in gas mixture. Two inlet conditions with LVF = 0.4% and 2.2%. Test data and CFD results in Ref. [11].

		Mixture [g/s]			Gas [g/s]			Oil [g/s]		
	At seal inlet	Code	TEST	CFD	Code	TEST	CFD	Code	TEST	CFD
P_S = 2.3 bar	LVF = 0.4% **(Liquid mass fraction =57%)**	27.8	27.2 ±3	28.4	12.0	11.7	12.3	15.8	15.5	16.1
P_S = 3.2 bar	Inlet LVF = 2.2% **(Liquid mass fraction =83.7%)**	68.6	68.7 ±3	69.3	10.9	11.2	11.0	57.7	57.5	58.3

Table 3 lists the current model predicted liquid volume fraction (LVF) and gas volume fraction (β), mixture specific heat ratio (γ_m), pressure at the seal inlet plane (P_e), mixture sound speeds, and gas, liquid and mixture Mach numbers at the inlet and outlet of the PDS. For a given condition, the mixture specific heat ratio (γ_m) is a constant through the seal as it is mass fraction weighted, see Eq. (8).

For both P_S = 2.3 bar and 3.2 bar, the pressure at seal inlet $P_e \sim 0.95\ P_S$ with an assumed ζ = 0.1. The sound speed in the mixture (a_m) is a small fraction of the liquid sound speed (a_l) and about 0.60 to 0.40 of the sound speed in the gas (a_g). Note a_m changes little across the seal for the two operating conditions, which is due to the large oil density and large liquid sound speed ($\rho_l\ a_l^2 \sim 1.8\times10^9$ [kg/(m·s)] >> $\rho_g\ a_g^2$) dominating Eq. (9). The changes of gas volume fraction (β), gas density (ρ_g) and mixture density (ρ_m) within the seal have a minor influence on the mixture sound

speed (a_m). For the two operating conditions, $Ma_m \sim 0.3$ at seal inlet, which indicates the oil and gas mixture is highly compressible. For P_S = 3.2 bar and at the seal outlet, Ma_m = 0.95, close to a choke condition.

Table 3. Current model predicted liquid volume fraction (LVF), gas volume fraction (β), mixture specific heat ratio (γ_m), seal inlet pressure (P_e), mixture sound speed (a_m) and Mach number at seal inlet and outlet planes for a PDS operating with an oil in gas mixture with inlet LVF = 0.4% and 2.2%.

	Inlet plane	Outlet plane
P_S = 2.3 bar (λ =43%)	**LVF = 0.4%** (β_S = 99.6%)	LVF = 0.2% (β = 99.8%)
	γ_m = 1.17	γ_m = 1.17
	P_e = 2.19 bar (P_e / P_S = 0.95)	-
	a_m = 235 m/s	a_m = 236 m/s
	Ma_g = 0.18, Ma_l = 0.04 Ma_m = 0.28	Ma_g = 0.42, Ma_l = 0.10 Ma_m = 0.64
P_S = 3.2 bar (λ=16.7%)	**LVF = 2.2%** (β_S = 99.6%)	LVF = 0.7% (β = 99.3%)
	γ_m = 1.06	γ_m = 1.06
	P_e = 3.04 bar (P_e / P_S = 0.95)	-
	a_m = 145 m/s	a_m = 142 m/s
	Ma_g = 0.12, Ma_l = 0.03 Ma_m = 0.30	Ma_g = 0.38, Ma_l = 0.09 Ma_m = 0.95

(Gas isothermal sound speed a_g = 356 m/s, liquid sound speed a_l = 1470 m/s)

Validation 3. Leakage for a PDS operating with a large pressure drop

Delgado and Thiele [6] report experimental results for an eight-blade, eight pocket fully partitioned PDS operating with supply pressure P_S = 70 bar, pressure ratio $PR = P_a / P_S$, and rotor speed up to 20 krpm (surface speed ΩR = 120 m/s). The PDS is supplied with a silicone oil in air mixture with gas volume fraction β_S = 0.90 ~ 1.0 (pure gas). Table 4 lists the geometrical dimensions and operating conditions for the test PDS.

A two-dimensional CFD model predicts the leakage and cavity pressures for the PDS operating with just gas (air) at a supply pressure P_S = 70 bar and rotor speed 10 krpm. The inlet gas volume

fraction $\beta_S = 1$. Details about the CFD analysis are not shown here for simplicity though given in an upcoming lecture [22].

Figure 11 shows the current model prediction, measured and CFD predicted leakage versus $PR = P_a / P_S$. The CFD predicted leakage is lower than the measurement; the maximum difference is ~ 9% for $PR = P_a / P_S = 0.65$. The current simple model prediction is lower than the CFD results for $PR \geq 0.3$. The difference between the measured flow magnitude and current model prediction amounts to no more than 16%. For $PR = 0.5$, the test leakage = 493.5 g/s. The current model predicted leakage = 416.4 g/s (~ 16% less) and CFD prediction = 448.3 g/s (~ 9% less).

Table 4. Geometry of an eight-blade, eight-pocket PDS and operating conditions. From Ref. [6].

Rotor diameter, $D = 2R$	114.6 mm
Seal length, L	85.7 mm
Clearance, C_r	0.203 mm
Number of blade (*ribs*)	8
Blades (*ribs*) thickness, δ	1.91 mm
Cavity length, L_c	13.34 mm and 5.72 mm
Cavity depth, d_c	3.65 mm
Number of ridges (circumferential)	8
Supply pressure, P_S	70 bar
Temperature, T_S	~ 290 K
Ambient pressure, P_a	17.5, 35, 45.5 bar
Rotor speed, Ω	10, 15, 20 krpm
Surface speed, ΩR	60, 90, 120 m/s
Inlet swirl ratio, α	0 ~ 1.3
Air density (at P_S and T_S), ρ_g	81.4 kg/m^3
Air viscosity (at T_S), μ_l	1.84×10^{-5} kg/(m·s)
Oil density (at P_S and T_S), ρ_l	910 kg/m^3
Inlet gas volume fraction, β_S	0.9, 0.92,.., 1.0 (gas)

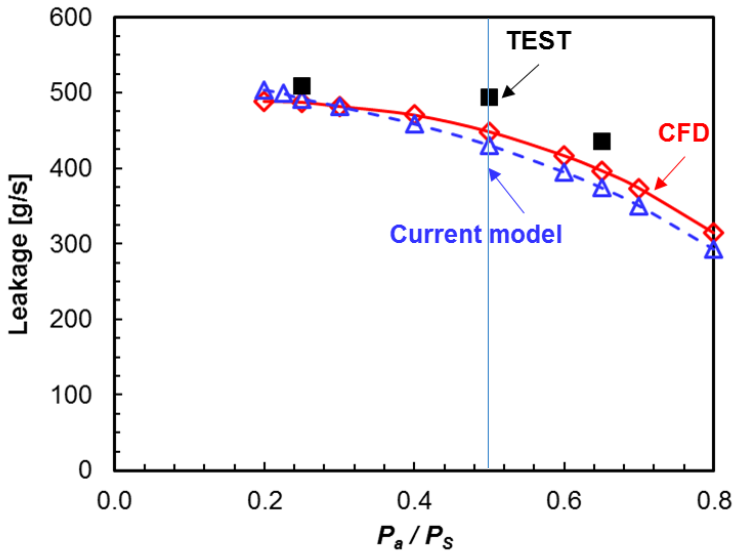

Figure 11. Air supplied PDS: current model prediction, measured and CFD predicted leakage vs *PR* = (P_a /P_S). Supply pressure = 70 bar, rotor speed 10 krpm (surface speed 61 m/s), medium inlet pre-swirl condition (α = 0.6 ~ 1.2). Test data from Ref. [6].

Validation 4. Leakage for a PDS operating with a large pressure drop and supplied with a mixture

For the PDS in Ref. [6] and supplied with an oil in gas mixture with inlet gas volume fraction β_S = 0.90 ~ 1.0, Figure 12(a) displays the current model predicted, measured and CFD predicted mass flow rates vs. inlet GVF, and Fig. 12(b) depicts the individual (liquid and gas) mass flow rates. Note the liquid mass fraction is as high as ~ 0.5 for β_S = 0.90 in the test result. The CFD analysis employs an Eulerian inhomogeneous two-phase flow model. An upcoming lecture will report more details about the CFD model [22].

The measured gas leakage has a jump (493.5 g/s → 586.1 g/s) when β_S = 1.0 drops to 0.98, then the measurements gradually decrease as β_S reduces to 0.90. Unlike the test data, the current model predicted and CFD predicted gas leakage decreases consistently with a decrease in β_S. The measurements appear to have a degree of uncertainty on the estimation of the air mass flow rate. The test oil leakage and the current model and CFD predictions increases linearly for β_S reduces from 1.0 to 0.90, while the test data has a larger magnitude than the two numerical predictions. The current model prediction and the CFD predictions are ~ 37% and ~ 33% (at maximum) less than the test results for β_S = 0.90 ~ 0.98, respectively.

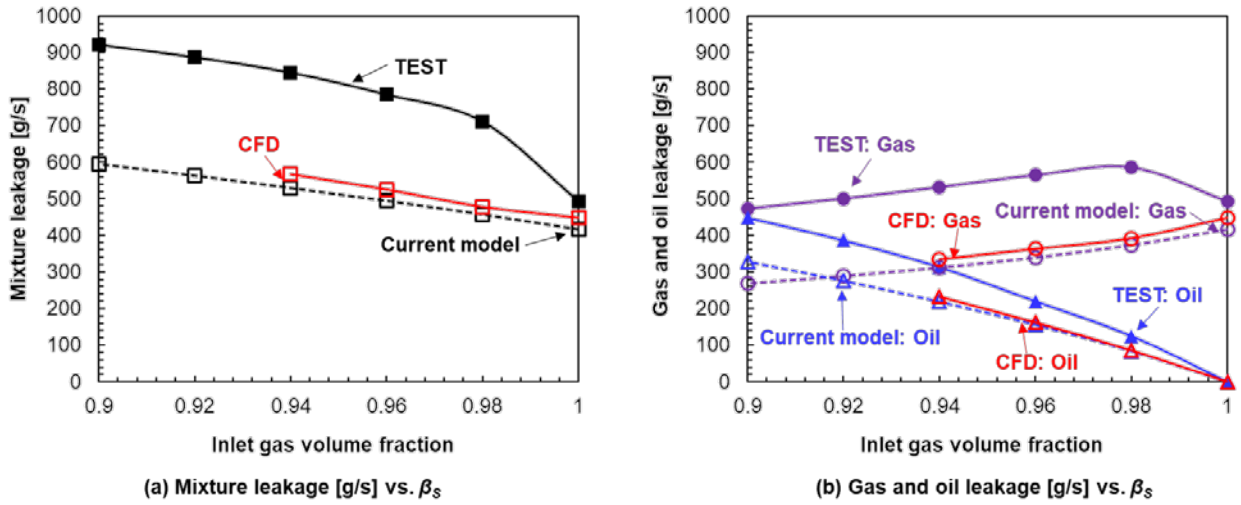

Figure 12. Current model predicted, measured and CFD predicted leakage for PDS operating with an oil / gas mixture vs inlet gas volume fraction (β_S). Supply pressure = 70 bar, pressure ratio *PR* = 0.5, rotor speed 10 krpm (surface speed 61 m/s), medium inlet pre-swirl condition. Test data from Ref. [6].

Figure 13 displays the outlet ($z=L$) gas volume fraction, and the predicted and measured gas mass fraction for the inlet gas volume fraction $\beta_S = 0.9 \sim 1$. Over the narrow range of GVFs shown, the outlet GVF grows linearly with β_S. For a given supply condition, the gas mass fraction is a constant through the seal. The predicted gas mass fraction is slightly lower than the test result, with a maximum difference ~ 12% at $\beta_S = 0.9$.

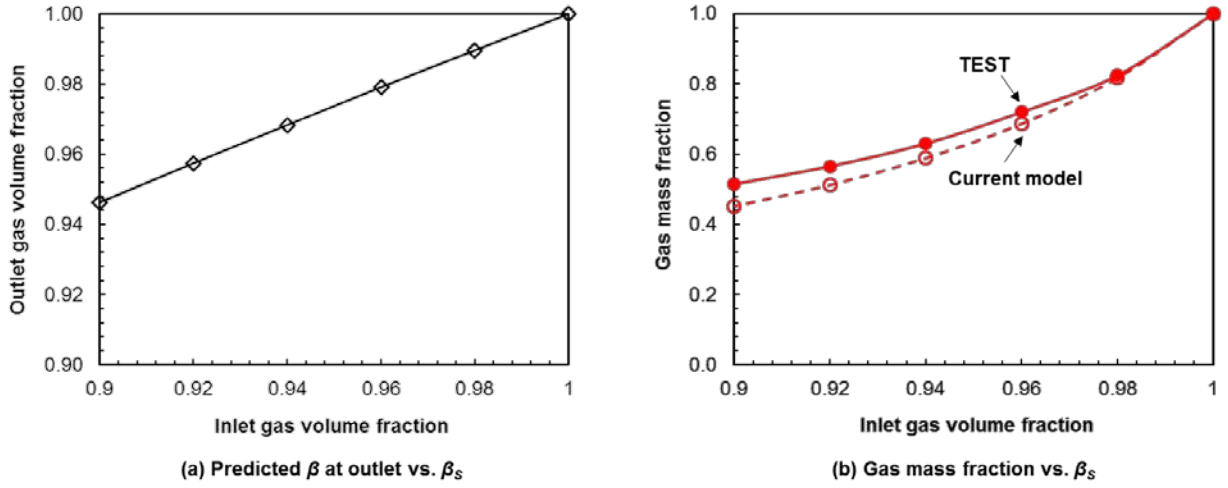

Figure 13. Current model predicted outlet gas volume fraction, and predicted and measured gas mass fraction vs inlet gas volume fraction (β_S). Supply pressure = 70 bar, pressure ratio *PR* = 0.5, rotor speed 10 krpm (surface speed 61 m/s), medium inlet pre-swirl condition. Test data from Ref. [6].

5. CONCLUSION

With the oil and gas industry moving towards subsea, compressors and pumps must withstand two-phase flows whose gas volume fraction (GVF) or liquid volume fraction (LVF) varies over a wide range during the operation of the well. A two-phase flow condition affects the leakage and dynamic forced performance of secondary flow components, namely seals, thus affecting the stability and reliability of pumping/compressing systems.

There are already bulk flow models (BFMs) for the prediction of leakage and dynamic performance for smooth surface, uniform clearance seals [12-15]. However, for ubiquituous labyrinth seals (LSs) and pocket damper seals (PDSs), a time-efficient analytical model is not yet available. The present work produced a simple tool for predicting the leakage and cavity pressure for both a labyrinth seal or a PDS operating with a liquid in gas mixture. A simple leakage formulation is derived from an adaptation of Neumann's leakage equation and using the physical properties of a homogeneous two-phase flow mixture.

The current model predicts the leakage and cavity pressure for a four-blade, eight-pocket PDS [11] operating with low supply pressure (P_S = 2.3 bar and 3.2 bar) and low rotor speed (Ω = 5,250 rpm, ΩR = 35 m/s). For both the pure gas and wet gas conditions, the predicted leakage agrees with the test data. The predicted cavity pressures deviate from the CFD predations, in particular for a choked flow condition (P_S = 3.2 bar).

For an eight-blade, eight-pocket PDS [6] supplied with air at a high supply pressure (P_S = 70 bar) and rotor speed at Ω = 10 krpm (ΩR = 61 m/s), the current model leakage prediction and a CFD prediction of leakage differ at most by 14 % and 9% with the measured leakage, respectively. For the PDS operating with an oil in gas mixture (inlet gas volume fraction β_S = 0.9 ~ 0.98) and pressure ratio PR = 0.5, the current model predicted and CFD predicted mass flow for the mixture are in good agreement, though they are ~ 37% and ~ 33% lower than the measurements respectively. The measured air mass flow rate in Ref. [6] is likely in error.

The current simple model (mixture flow) predictions are accurate when compared to test data for both a low pressure PDS and a high pressure PDS.

The following work will contemplate the development of a BFM prediction of the force coefficients of *wet* gas LSs and PDSs. The new BFM will employ a two-component flow homogeneous mixture model to perform the prediction. The predictions by the two-phase flow BFM will validate against the test data and CFD predictions for *wet* gas PDSs and LSs.

ACKNOWLEDGMENTS

The authors are grateful to the Turbomachinery Research Consortium (TRC) for the financial supports.

NOMENCATURE

C_r	Seal radial clearance [m]
D	2R. Rotor diameter [m]
L	Seal land length [m]
L_C	Pocket length [m]
Ma	Mach number [-]
$\dot{m}$	Leakage (mass flow rate) [kg/s]
P	Static pressure [Pa]
P_e	Static pressure at the seal inlet [Pa]
P_S, P_a	Supply and discharge pressures [Pa]
R	Rotor radius [m]
R_g	Air constant, R_g = 287 J/(kg·K)
T_S	Temperature of supply fluid [K]
W, U	Axial velocity and circumferential velocity [m/s]
α	Inlet pre-swirl ratio [-]
β	Gas volume fraction [-]
λ	Gas mass fraction [-]
γ	Specific heat ratio [-]
μ	Dynamic viscosity [Pa·s]
μ_c	Kinetic energy carry-over coefficient, Eq. (12)
μ_f	Flow discharge coefficient, Eq. (13)
ω	Whirl frequency [rad/s]
Ω	Rotor angular velocity [rad/s]
ρ	Density, [kg/m^3]

Abbreviations

BFM	Bulk flow model
CFD	Computational Fluid Dynamics
LS	Labyrinth seal
PDS	Pocket damper seal

Subscripts

g	Gas
l	Liquid
m	Gas and liquid Mixture

REFERENCES

[1] Vance, J. M., and Shultz, R. R, 1993, "A New Damper Seal for Turbomachinery," Proc. of the 14th Vibration and Noise Conference, September 19-22, Albuquerque, NM, ASME DE-60, pp. 139-148.

[2] Vannini, G, Bertoneri, M., Del Vescovo, G., Wilcox, M., 2014, "Centrifugal Compressor Rotordynamics in Wet Gas Conditions," Proc. of the Turbomachinery & Pump Symposium, September 22-25, Houston, TX, pp. 201-220. Available electronically from http: / /hdl .handle .net /1969 .1 /162697.

[3] Vannini, G., Bertoneri, M., Nielsen, K. K, Ludiciani, P., and Stronach, R., 2016, "Experimental Results and Computational Fluid Dynamics Simulations of Labyrinth and Pocket Damper Seals for Wet Gas Compression," ASME J. Eng. Gas Turbines Power, **138**(5), pp. 052501.

[4] Zhang, M., James, E., Mclean, Jr., and Childs, D., 2017, "Experimental Study of the Static and Dynamic Characteristics of a Long Smooth Seal with Two-Phase, Mainly-Air Mixtures," ASME J. Eng. Gas Turbines Power, **139**(12), pp. 122504.

[5] Zhang, M., Childs, D., Mclean, J. E., Jr., Tran, D. L., and Shrestha, H., 2019, "Experimental Study of the Leakage and Rotordynamic Coefficients of a Long Smooth Seal with Two-Phase, Mainly-Oil Mixtures," ASME J. Tribol., **141**(4), pp. 042201.

[6] Delgado, A., and Thiele, J., 2019, "Rotordynamic Characteristics of Fully Partitioned Pocket Damper Seal," Turbomachinery Research Consortium (TRC) Progress Report, Texas A&M University, College Station, TX.

[7] San Andrés, L., Lu, X., and Liu, Q., 2016, "Measurements of Flow Rate and Force Coefficients in a Short-Length Annular Seal Supplied With a Liquid/Gas Mixture (Stationary Journal)," Tribol. Trans., **59**(4), pp. 758–767.

[8] San Andrés, L., and Lu, X., 2017, "Leakage, Drag Power and Rotordynamic Force Coefficients of an Air in Oil (Wet) Annular Seal," ASME J. Eng. Gas Turbines Power, **140**(1), pp. 012505.

[9] San Andrés, L., and Lu, X., 2018, "Leakage and Rotordynamic Force Coefficients of a Three-Wave (Air in Oil) Wet Annular Seal: Measurements and Predictions," ASME J. Eng. Gas Turbines Power, **141**(3), pp. 032503.

[10] San Andrés, L., Lu, X., and Jie, Z., 2018, "On the Leakage and Rotordynamic Force Coefficients of Pump Annular Seals Operating With Air/Oil Mixtures: Measurements and Predictions," Second Asia Turbomachinery and Pump Symposium, The Turbomachinery Laboratory, Texas A&M University, Singapore, March 13–15.

[11] Yang, J., San Andrés, L., and Lu, X., 2019, "Leakage and Dynamic Force Coefficients of a Pocket Damper Seal Operating Under a Wet Gas Condition: Tests VS. Predictions," ASME J. Eng. Gas Turbines Power, **141**(11), pp. 111001.

[12] San Andrés, L., 2012, "Rotordynamic Force Coefficients of Bubbly Mixture Annular Pressure Seals," ASME J. Eng. Gas Turbines Power, **134**(2), pp. 022503.

[13] Arghir, M., Zerarka, E., and Pieanu, G., 2011, "Rotordynamic Analysis of Textured Annular Seals with Multiphase (Bubbly) Flow," INCAS Bull., **3**(3), pp. 3–13.

[14] Grimaldi, G., Pascazio, G., Vannini, G., and Afferrante, L., 2019, "Stratified Two-Phase Flow in Annular Seals," ASME J. Eng. Gas Turb. Power, **141**(7), pp. 071006.

[15] San Andrés, L., Lu. X., 2020, “A Nonhomogeneous Bulk Flow Model for Prediction of the Static and Dynamic Forced Performance of Two Phase Flow Annular Seals,” TRC-SEAL-02-2020, Turbomachinery Research Consortium (TRC) Final Report, Texas A&M University, College Station, TX.

[16] Cicchitti, A., Lombaradi, C., Silversti, M., Soldaini, G., Zavattarlli, R., 1960, “Two-Phase Cooling Experiments – Pressure Drop Heat Transfer Burnout Measurements,” Energia Nucleare, **7**(6), pp. 407–425.

[17] Fourar, M., Bories, S., 1995, “Experimental Study of Air-Water Two-Phase Flow through a Fracture (Narrow Channel),” Int. J. Multiphase Flow, **21**, pp. 621-637.

[18] Neumann, K., 1964, “Zur Frage der Verwendung von Durchblickdichtungen im Dampfturbinenbau,” Maschinentecknik, **13**(4).

[19] Childs, D. W., 1993, *Turbomachinery Rotordynamics: Phenomena, Modeling, and Analysis*, Chapter 5, “Rotordynamic Models for Annular Gas Seals,” John Wiley & Sons.

[20] Arghir, M, and Frene, J., 2001, “Numerical Solution of Lubrication’s Compressible Bulk Flow Equations. Applications to Annular Gas Seals Analysis,” ASME Paper No. 2001-GT-0117.

[21] Li, J., San Andrés, L., and Vance, J. M, 1999, “A Bulk-Flow Analysis of Multiple-Pocket Gas Damper Seals,” ASME J. Eng. Gas Turbines Power, **121**(4), pp. 355-363.

[22] Delgado, A., San Andrés, L., Jonathan, T., Yang, J., and Cangioli, F., 2020, “Rotordynamic Performance of a Fully-Partitioned Damper Seal: Experimental and Numerical Results,” Turbomachinery & Pump Symposia, September 14-17, Houston, TX.